Egyptian Journal of Petroleum (2016) 25, 281–291

HOSTED BY

ELSEVIER

Egyptian Petroleum Research Institute

Egyptian Journal of Petroleum

www.elsevier.com/locate/egyjp
www.sciencedirect.com

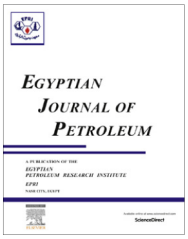

FULL LENGTH ARTICLE

# High performance nature of biodegradable polymeric nanocomposites for oil-well drilling fluids

**Tarek M. Madkour** [a], **Samar Fadl** [a], **M.M. Dardir** [b,*], **Mohamed A. Mekewi** [c]

[a] *Department of Chemistry, The American University in Cairo, New Cairo 11835, Egypt*
[b] *Drilling Fluids Laboratory – Production Department, The Egyptian Petroleum Research Institute, EPRI, Egypt*
[c] *Department of Chemistry, Faculty of Science, Ain-Shams University, Cairo, Egypt*

Received 21 May 2015; revised 30 August 2015; accepted 2 September 2015
Available online 22 December 2015

**KEYWORDS**

Polymeric nanocomposites;
Poly(lactic acid) (PLA);
Drilling fluids

**Abstract** Multi-walled carbon nanotube (MWCNT) and graphene nanoplatelet reinforced thermoplastic poly(lactic acid) (PLA) biodegradable nanocomposites were designed and prepared using solution casting techniques. The prepared biodegradable polymers are expected to provide an environmentally friendly alternative to petroleum-based polymers. Both nanocomposite systems exhibited better thermal stability and improved mechanical performance over the unreinforced polymer exhibiting excellent strength and degradability. The addition of graphene nanofiller in varied amounts was aimed to enhance the thermal and mechanical properties of the nanocomposites even further and incorporate the outstanding characteristics of graphene nanoplatelets into the nanocomposites. The polymeric nanocomposites showed also superior advantages for oil drilling relevances, automotive lubricating purposes, membrane technology and food packaging. Scanning electron microscopy images indicated a homogeneous dispersion of the nanofiller within the polymeric matrix at low filler loadings and a cluster formation at higher loadings that could be responsible for the polymeric matrix movement restrictions. The enthalpy of mixing (the polymer and the nanofiller) measured could explain the cause of the repulsive interactions between the nanoparticles and the polymeric chains, which created an additional excluded volume that the polymeric segments were restricted to occupy, thus forcing the conformational characteristics of the polymeric chains to deviate away from those of the bulk chains. The prepared polymeric nano composites (poly lactic acid carbon nano tube and poly lactic acid graphene nanoplatelets) were utilized in the formulation of oil-base mud as a viscosifier. The rheological, filtration properties and electrical stability of the oil based mud formulation with the new polymeric nanocomposite were studied and the result compared to the oil-based mud formulation with commercial viscosifier.



## 1. Introduction

The majority of plastic materials used nowadays are based on fossil raw materials. Packaging materials are produced in huge

* Corresponding author.
E-mail address: monamdardir@yahoo.com (M.M. Dardir).
Peer review under responsibility of Egyptian Petroleum Research Institute.

http://dx.doi.org/10.1016/j.ejpe.2015.09.004

amounts yearly and they are discarded after the product has been used, which contributes to growing landfills and enhanced greenhouse effects [1]. Due to the limited fossil fuel resources and the impact of petroleum-based materials on the environment, there is a huge undertaking by scientists and engineers to replace those materials by biological alternatives, which indicates the ongoing trend of a sustainable development in the near future [2]. The use of bio-nanocomposites for oil drilling, automotive lubricating purposes, membrane technology and food packaging has the potential to provide an environmentally friendly solution since it helps in the management of the world's waste problem and reduces the requirement for using petroleum-based plastics as packaging materials [3]. Most of the traditional petroleum-based packaging materials are made from non-degradable materials, which also increase environmental pollution in addition to consuming fossil fuels for their production. However, alternative biodegradable films are currently exhibiting poor barrier and mechanical properties, which need to be improved considerably before they are considered as a sound replacement for traditional plastics [4]. However, there are major concerns regarding the mechanical, thermal and barrier properties of the natural biopolymer-based packaging materials [5]. One way to improve the quality of these biodegradable and biorenewable polymers is to use nanocomposites based on these natural polymers that exhibit improved mechanical, thermal and gas barrier properties [6–8]. In an attempt to overcome these limitations, nanoclays have been used as supportive filling agents in a biopolyester matrix where they formed nanocomposite structures [9–11]. Cabedo et al. [9] showed that the addition of nanoclay such as kaolinite nanofillers to PLA films improved both their thermal stability and mechanical properties without decreasing barrier properties. The most important properties of materials are mechanical properties, thermal properties and gas barrier properties. Biodegradable polymers can be recovered through composting and returned to nature [12].

In recent years, composting is considered as the preferred method of treatment of organic solid waste, and this is where the biodegradable/compostable bioplastics are supposed to end up. Hence, compostable polymers especially derived from renewable resources are being promoted and known as environmentally beneficial materials for various industries [12]. It is challenging to be able to replace the conventional materials with bio-based ones. Another challenge is biodegradability which has to perform efficiently on disposal. Degradability can on one hand constrain biopolymer applications to short-term use, and on the other hand facilitate composting. There are several factors, such as water activity, microorganisms, temperature, composition of biomaterial, etc., which affect biodegradation as well as deterioration rate and must be considered in the various applications.

Biopolyesters have promising properties such as excellent transparency and cellophane-like mechanical properties. Blown films in commercial use are developed based on biodegradable polyesters, which do not contain six-carbon rings known as aliphatic polyesters such as poly(caprolactone) (PCL), poly(glycolic acid) (PGA) and poly(butylene succinate) (PBS). However, regarding the other requirements of a barrier film, it is believed that no single bio-based polymer can be both water vapor and gas barrier. Therefore, in this case, the use of co-extrusion can lead to laminates which meet the requirements [13]. Another class of products is thermoformed polymers. In order to thermoform a polymer, there should be a possibility to process the material from the melt (extrusion) into sheets and to thermoform the sheets just above the softening temperature of the material. Possible examples are biopolymers based on PLA and PHB/V (Poly Hydroxy Butyrate/Valerate), paragon laminates and also other thermoplastically processable biopolymers. Gas barriers of packaging materials become essential when the gas composition inside the package has to be kept constant [14–19]. The gas combination of packaging products is mostly $CO_2$, $O_2$ and $N_2$. There are also products that require specific atmospheric conditions during storage; therefore, they are packed in protective atmosphere with specific mixture of gases. Hence, the permeability of oxygen and other gases, which are closely interrelated, must be engineered and are desired to be low [19]. A material with lower oxygen permeability (OP) than 10 $cm^3.\mu m/m^2.day.kPa$ is considered to be a good oxygen barrier [15]. Many polysaccharides (natural polymeric carbohydrates) are known to be good oxygen barriers, explained by their hydrogen-bonded network which leads to small free volume that makes the oxygen transmission low [16]. In fact, biopolymers are able to mimic the oxygen permeability of a wide range of the conventional petroleum-based materials [17,18]. Humidity is another important parameter interfering in gas barrier properties. With increasing humidity gas permeability increases for both bio-based polymers and conventional ones, even high gas barrier materials such as nylon and ethylvinyl alcohol have a lower barrier performance in humid conditions. In order to manufacture appropriate materials for various applications, it is unlikely that just one polymer can have all properties. Therefore, employing multiple materials in a composite or use of nanocomposites might be necessary, which can fulfill high demands such as very low gas permeability, high water resistance, etc. A similar multi-layer approach can also be used for bio-based polymers.

Drilling fluids or drilling muds are an essential and a key component of the rotary drilling process used to drill for oil and gas on land and in offshore environment. The most important functions of drilling fluids are to transport cutting to the surface, to balance subsurface, cool, lubricate and support part of the weight drill bit and drill pipe [20–25]. Although the high toxicity of oil-based mud it is used when drilling deep wells due to its high performance and high thermal stability than water based-mud and also it is less expensive than synthetic based mud. Oil-based muds (OBM) don't hydrate the shell and maintain hole stability wells drilled with OBM which normally produce lower waste values than those drilled with water-based muds (WBM) because a nearly gauge hole is drilled and the mud is conditioned. Oil-based muds which are formulated with crude oil or diesel oil are excellent for inhibiting water – sensitive shell and clays extended reach – wells, highly density formation and drilling through salt [26–28].

Most oils lack many qualities necessary in drilling operations, for example, most crude petroleum oils of low density are inflammable, leading last the permeable formations and lack the required viscosity and gel strength property. Numerous means usually involve adding materials such as blown asphalt or other finely divided solids to the oil to increase the density, viscosity and gel strength and to give the fluid plastering properties to decrease loss of the fluid to permeable formation. Most of these materials are viscosifiers agent. The term oil-base drilling fluids has been as a system, the

continuous or external phase of which is any suitable oil. It may contain some water in the form of small homogenous in size and uniformly dispersed droplets commonly called the internal or discontinuous phase. Oil-base drilling fluids consist of a suitable oil, asphalt, water, calcium chloride, suspended solid (viscosifier) and emulsifiers [29,30]. Nano materials are considered to be the most promising matter of choice for drilling fluids designed for oil and gas field application. They can promote the development of drilling fluid technology effectively, so they have potential and bright prospect in oil and gas exploration and development. They have been widely used in the field of design and development of new drilling fluids. Some nano materials such as nano composite filtration – reducing agent, nano composite viscosifier, nano sized emulsion lubricant, and nano meter organo clay [31] The prepared polymeric nano composites (poly lactic acid carbon nano tube and poly lactic acid graphene nanoplatelets) showed good results when utilized in the formulation of oil-based mud as a viscosifier.

## 2. Methodology

### *2.1. Solution casting of the bionanocomposites*

Various bionanocomposites based on polylactic acid (PLA) and non-functionalized and functionalized multi-walled carbon nanotubes (NWNT) and graphene nanoplatelets (GNP) were prepared by solution casting. In all combinations, the formulation contained 0.5% by mass nanofiller. The solution casting of the bionanocomposite films was done by dissolving 20 grams of the biopolyesters supplied locally in 600 ml tetrahydrofuran supplied from Sigma–Aldrich followed by the addition of the nanofillers supplied from CheapTubes and were mixed for 24 h with continuous stirring. After complete mixing, the solvent was allowed to evaporate and the resultant nanocomposites were ready for testing.

### *2.2. Scanning electron microscopy (SEM)*

SEM (SUPRA 55 LEO SEM, a high resolution FEGSEM) was used for the analysis of the materials to examine the distribution of the nanoparticles within the polymeric matrix and for mapping the crystal orientation, if any, of the materials.

### *2.3. Stress relaxation measurements*

The stress–strain isotherms of the various PU samples at room temperature were obtained on dumbbell-shaped specimens cut from the molded nanocomposite sheets to evaluate the mechanical response of the nanocomposites and the influence of the inclusion of the nanoparticles on the mechanical behavior of the samples according to:

$$[f^*] = f/[A^*(\alpha - \alpha^{-2})] \quad (1)$$

where $[f^*]$ is the modulus, $A$ is the cross-sectional area and $\alpha$ is the elongation.

### *2.4. Mud formulation*

The materials and chemical additives of oil-based mud were obtained from the Baroid company to be used as a reference sample.

The mud formulation was prepared according to API, OCMA specification [32,33].

Work for oil-based mud with an oil–water ratio (70/30).

The formulation was performed by using a new polymeric nano composite carbon nano tube (C) and polymeric nano composite graphene nanoplatelets (G) as viscosifiers compared to the commercial viscosifier (R) from the Baroid company. The formulation of the oil-based mud consists of:

Diesel oil 375 ml + primary emulsifier (10 ml) + tab water (125 ml) + viscosifier (1.99%) 8.5 g + organic surfactant (1.59%) 6.8 g + soda (1.59) 6.8 g + supplementary emulsifier (5 ml).

So we have three mud batches:

MR: mud formulation of oil- based with the commercial viscosifier (R).
MC: mud formulation of oil- based and treated with polymeric nano composite (C).
MG: mud formulation of oil-based and treated with the polymeric nano composite (G).

Rheological properties, High pressure High temperature filter loss test, electrical stability, were carried out to each of the three formulated mud batches and the effect of temperature on the rheological properties.

## 3. Rheological properties

Apparent viscosity (AV), plastic viscosity (PV), and yield point (YP) were determined by making a relation between shear rate and shear stress, where the shear rate was taken from the dial reading which is in degree of a circle.

Shear rate, sec-1 = rpm × 1.7034.
Apparent viscosity (AV), cp = reading at 600 rpm/2.
Plastic viscosity (PV) cp = reading at 600 rpm − reading at 300 rpm.
Yield point (YP) lb/100 ft2 = reading at 300 rpm − plastic viscosity.

Viscosity of the mud is a function of temperature more than pressure. Commonly, it is necessary to measure viscosity at elevated bottom hole temperature. This is done by using the viscometer cupheater, Chandler Engineering Laboratory Model API viscometer (Chan 35 Model 3500), which is a thermostatic-controlled unit for heating the mud sample directly on a viscometer.

### *3.1. Determination of gel strength and thixotropy of a mud*

The gel strength of the mud is a measure of a minimum shearing stress necessary to produce slip-wise movement of fluid. Two readings are generally taken, immediately after agitation of the mud in the cup (10 s) and after the mud in the cup has been rested for 10 min.

*3.2. High pressure–high temperature filter loss*

The test was carried out by using standard HP-HT filter loss Model 107ıC. The experiment was run at 300ıF and 500 psi and the volume of filtrate reading recorded from the graduated cylinder at the end of 2, 5, 10, 15, and 30 min.

## 4. Electric stability

A fan apparatus Model 23D was used to indicate the electrical stability of the mud.

## 5. Results and discussion

*5.1. Characterization of the nanocomposite samples*

All the nanocomposite samples have already been characterized using fourier transform infrared (FTIR), differential scanning calorimetry (DSC) and thermal gravimetric analysis (TGA) techniques as descried in previous work (33), it is worth mentioning that for all samples, the addition of the nanofillers didn't influence the thermal behavior of the polymeric matrix in which the filler particles were incorporated as studied using TGA and DSG techniques, additionally, the FTIR profile, didn't show any changes as a result of the addition of the nanoparticles to polymeric material.

It was thus concluded that the addition of the nanofiller particles didn't lead to any chemical or morphological changes of the polymeric chains.

*5.2. Scanning electron microscopy (SEM)*

SEM micrographs of 0.5% by mass of non-functionalized and functionalized CNT and GNP-reinforced PLA nanocomposites are shown in Figs. 1–4, respectively. It is observed that the nanofillers are well-dispersed in a good order within the


**Figure 1** SEM micrograph of non-functionalized CNT-filled PLA nanocomposite.

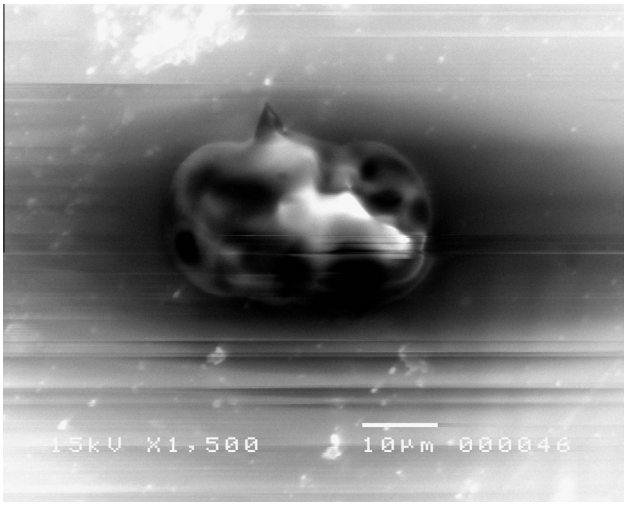


**Figure 3** SEM micrograph of non-functionalized GNP-filled PLA nanocomposite.

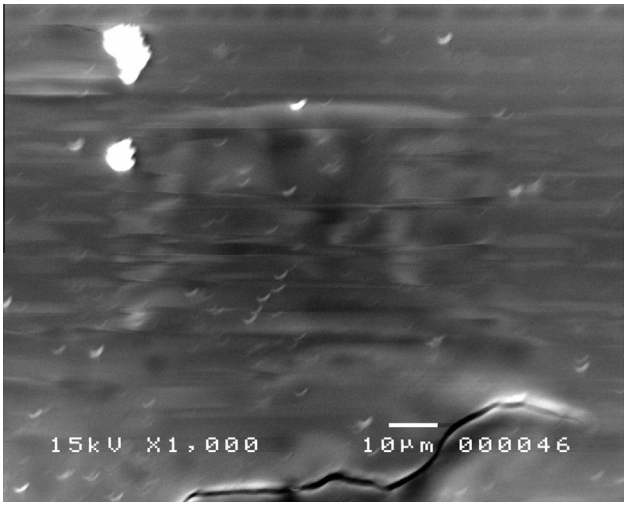


**Figure 2** SEM micrograph of functionalized CNT-filled PLA nanocomposite.

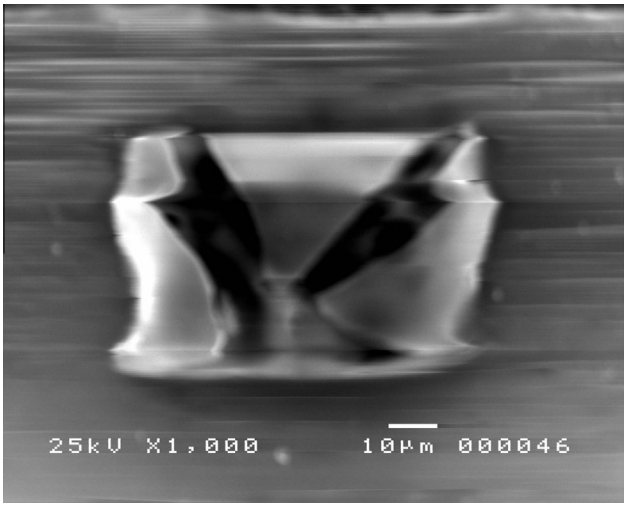


**Figure 4** SEM micrograph of functionalized GNP-filled PLA nanocomposite.

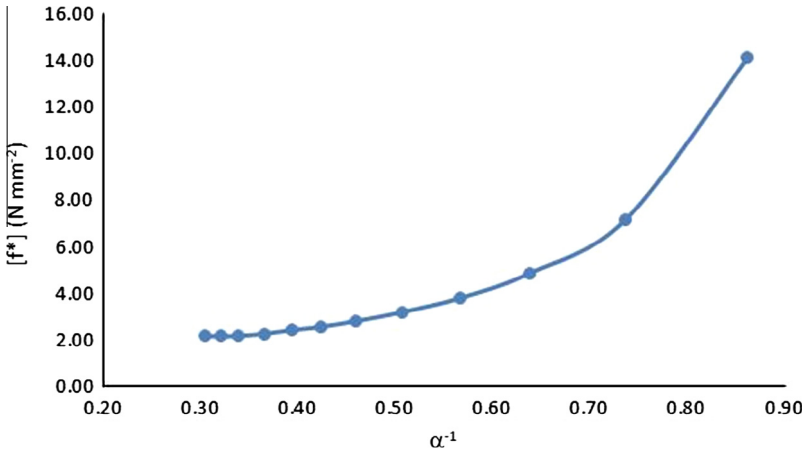


**Figure 5** Stress–Strain isotherm for the non-reinforced poly(lactic acid).

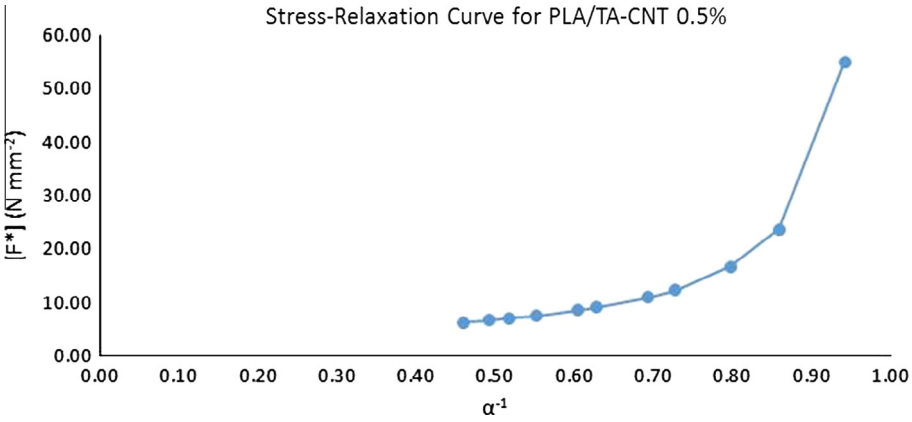


**Figure 6** Stress–Strain isotherm for the non-functionalized CNT-reinforced poly(lactic acid).

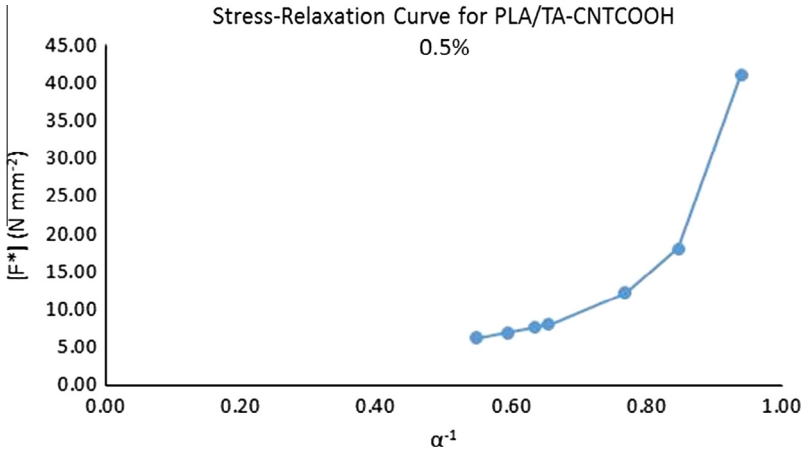


**Figure 7** Stress–Strain isotherm for the functionalized CNT-reinforced poly(lactic acid).

polymeric matrix. From the SEM images shown in Fig. 2, one can clearly observe that most of the functionalized CNT nano-filler embedded within the polymeric matrix have a bending behavior with different bending angles. This is quite interesting since this behavior is not observed for the non-functionalized ones shown in Fig. 1, which appeared straight in the SEM image.

This could be attributed to the formation of hydrogen bonding between the hydroxyl groups of the carboxylic functional group on the surface of the CNT particles and the

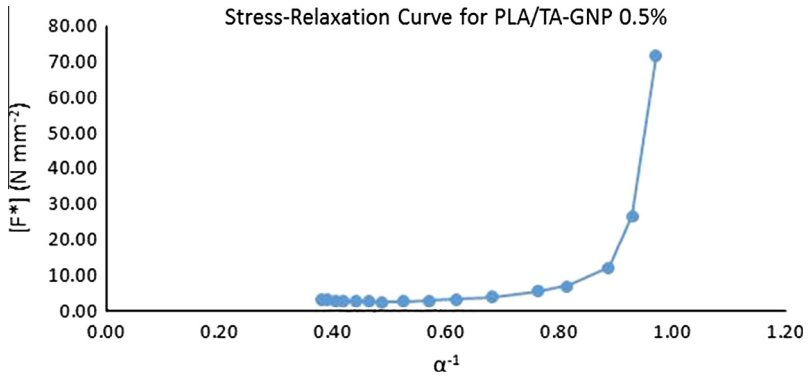


**Figure 8** Stress–Strain isotherm for the non-functionalized GNP-reinforced poly(lactic acid).

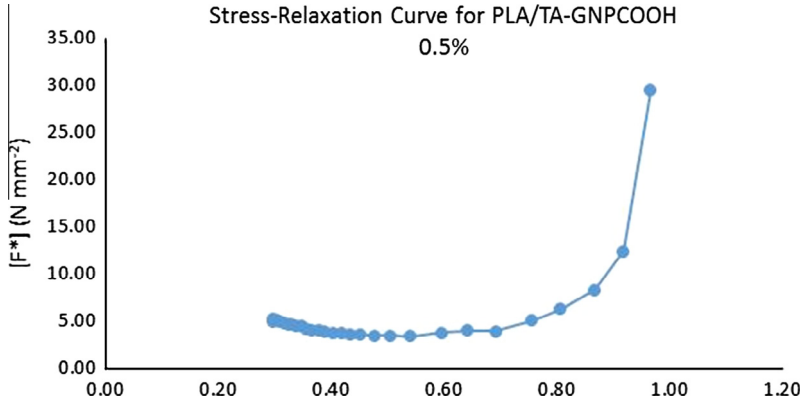


**Figure 9** Stress–Strain isotherm for the functionalized GNP-reinforced poly(lactic acid).

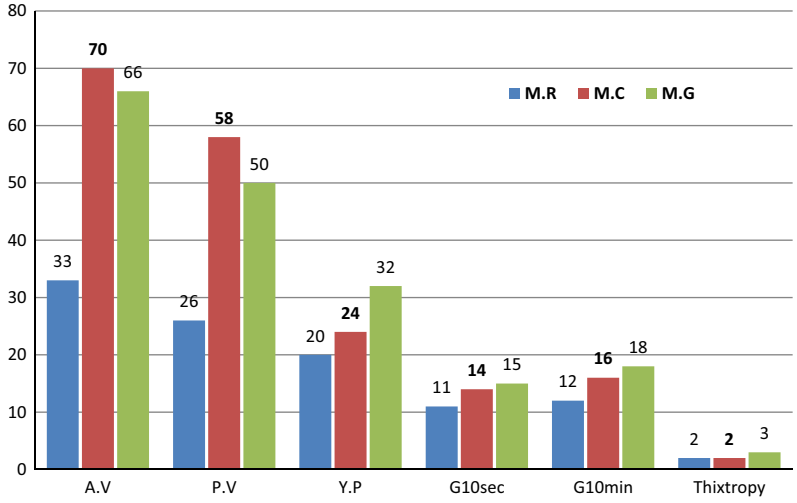


**Figure 10** Rheological properties, gel strength and thixotropy of the oil-based mud formulated by the new viscosifiers.

carbonyl oxygen of the ester group of PLA. This not only has the potential of locking the nanoparticle in place within the polymer matrix but also applying enough stress on the nanofiller particles causing the particle to yield and resulting in the observed bending behavior.

Same conclusion may also be drawn when comparing the functionalized graphene nanoplatelets to the non-functionalized one but to a much lesser extent due to the massive surface area of the nanoplatelets as compared to the nanotubes.

### *5.3. Stress relaxation and hardness measurements*

The representation of the stress–strain data was based on the Mooney-Rivlin equation:

$$[f^*] = 2C_1 + 2C_2\alpha^{-1} \quad (2)$$

where $2C_1$ and $2C_2$ are constants. Typical isotherms of this type are shown in Figs. 5–9 for the non-reinforced polymer, the non-functionalized and functionalized CNT and GNP-reinforced PLA nanocomposites, respectively. Every isotherm in the figure represents the stress–strain behavior of each one of the investigated samples. The results shown in Figs. 5–9 clearly demonstrate the apparent enhancement in the mechanical performance of the nanofilled PLA nanocomposites over those of the neat polymer. Interestingly, samples incorporating non-functionalized nanofillers showed at least four fold increment in the modulus values as compared to that of the neat polymer while showing a decrease in the elongation values possibly due to the apparent stiffening of the polymeric chains. For the functionalized nanofilled samples, the increase in the modulus values was only two fold, which still is a remarkable improvement in the mechanical strength of the samples. Two interesting observations were made in the functionalized GNP-reinforced PLA sample. Firstly, while the modulus has doubled in value due to the incorporation of the graphene nanoplatelets indicating a greater strength of the polymeric chains, the elongation has remained the same as compared to the neat polymer. This indicates that the observed increase in the polymer strength has not affected its elasticity or flexibility. Secondly, according to Eq. (2), the modulus of the samples should decrease with an increase in the elongation. This did occur until high strains were reached. Instead of continuing to decrease, an upturn in the modulus values was obtained. This "non-Gaussian" behavior of the sample would consequently explain the observed toughness at high elongations and unusual high energy levels are required to reach the maximum stress. The observed mechanical performance of the nanocomposites depends not only on the functionalization of the nanotubes, but also on the presence of the nanoscale CNTs impeded within the polymeric matrix. These observations can be explained by considering the confinement of the polymeric chains between the large numbers of the nanofiller particles scattered around, which restricts the movement of the polymeric chains greatly and thus diminishing the number of configurational states accessible to the chains and resulting in a significant decrease in the entropy of the chains and a corresponding increase in the elastic moduli.

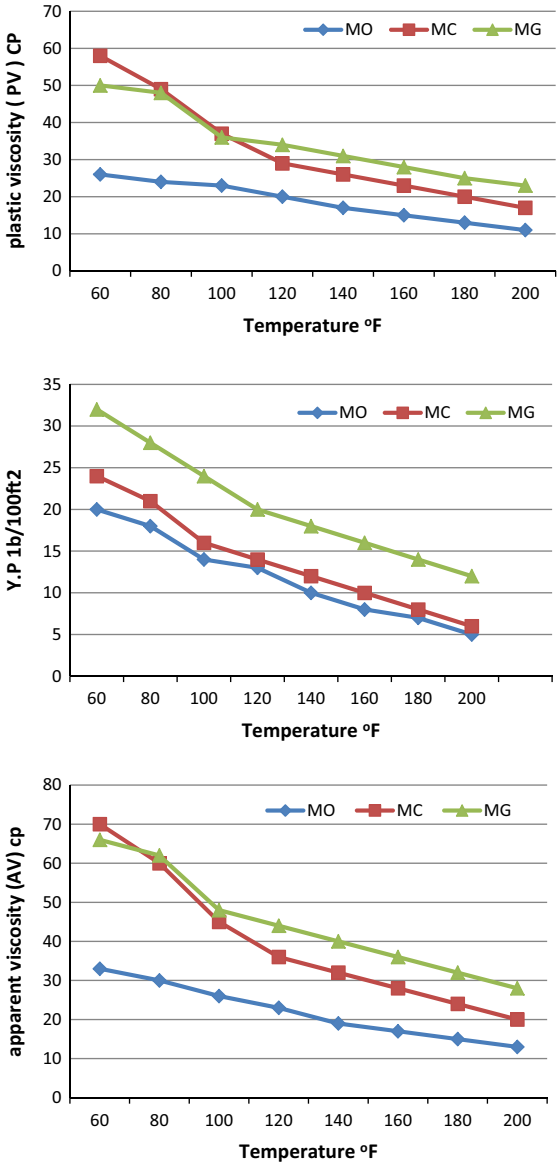


**Figure 11** Rheological properties–temperature relationship of MC, MG compared to MR.

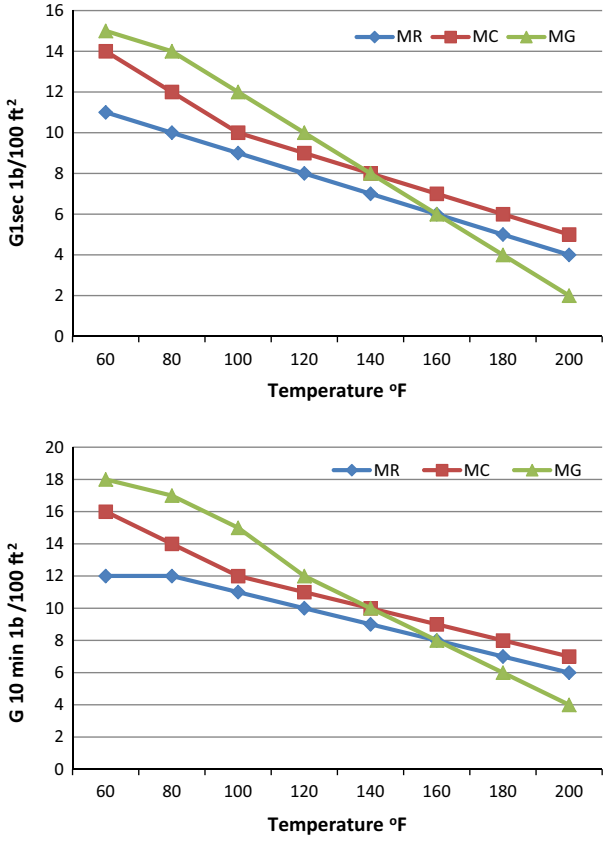


**Figure 12** Gel strength–temperature relationship of MC, MG compared to MR.

## 6. Evaluation

Evaluation of the polymeric carbon nano composite (C) and polymeric graphene nanoplates (G) as a viscosifier in oil based mud compared to the commercial viscosifier (R). The oil-based mud formulation contains oil/water (70/30) and 1.99% imported viscosifier for utilization in oil-well drilling fluids. This formulation was considered as the control sample (reference) for the evaluation measurements of the new viscosifier. In this research the evaluation incorporates the following:

**Table 1** Thixotropy–temperature relationship.

| Temperature °F | MR | MC | MG |
|---|---|---|---|
| 60 | 1 | 2 | 3 |
| 80 | 2 | 2 | 3 |
| 100 | 2 | 2 | 3 |
| 120 | 2 | 2 | 2 |
| 140 | 2 | 2 | 2 |
| 160 | 2 | 2 | 2 |
| 180 | 2 | 2 | 2 |
| 200 | 2 | 2 | 2 |

### 6.1. Rheological properties

The rheological properties of oil-based mud, treated with the prepared nano composite (C) and (G) were measured compared to the field oil-based mud formulated by the commercial viscosifier (R) as a reference sample. Rheological results are illustrated in Fig. 10 and showed that: apparent viscosity of the oil based mud formulated by the prepared nano composite was 70 cp and 66 cp for both MC and MG which are more than the apparent viscosity of MR (33 cp).

*Plastic viscosity*: the plastic viscosity was 58 and 50 cp for both MC and MG where for MR was 26 cp.

*Yield point*: the yield point was 24 and 32 (1b/100 ft2) for both MC and MG where for MR was 20 (1b/100 ft2). From the above result we conclude that the rheological properties of the oil-based mud formulated with the prepared polymeric nanocomposite were compatible with the API specification and have great value than the oil-based mud formulated with the commercial viscosifier.

*Gel strength*: The gel strength and thixotropy of the oil-based muds formulated with the new prepared polymeric nano composite C and G are plotted in Fig. 10 compared to the reference viscosifier in oil-filled mud; their values change from 14,

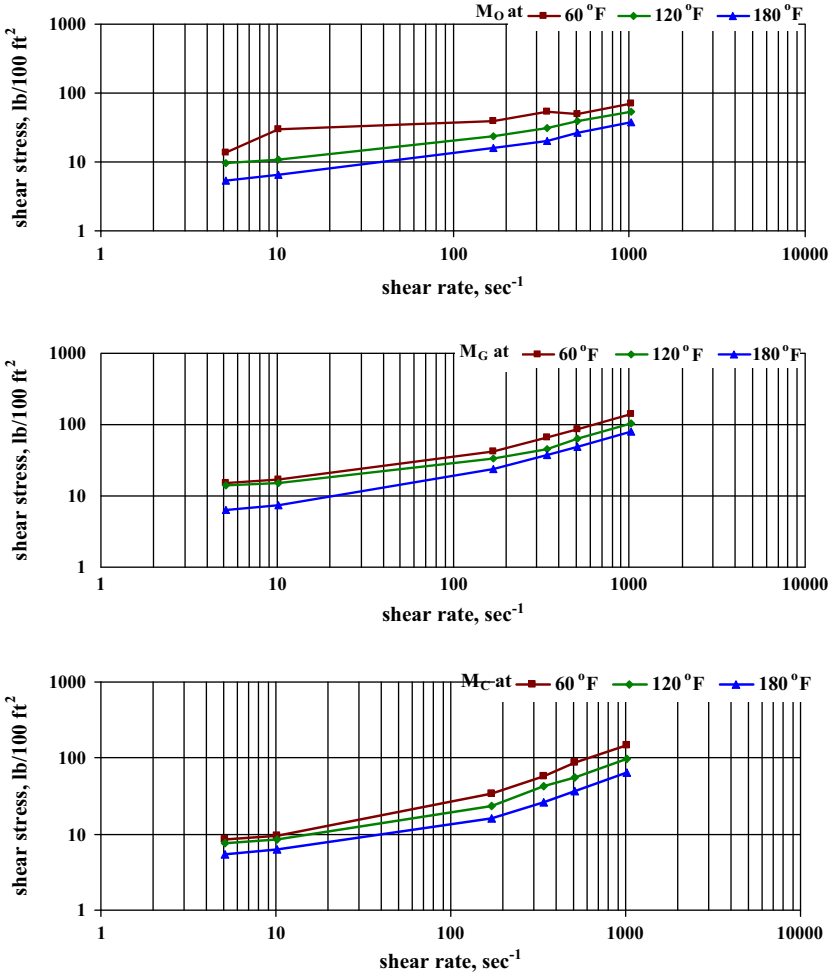


**Figure 13** Shear rate–shear stress relationship of $M_o$, $M_G$ and $M_C$ at 60 °F, 120 °F and 180 °F.

15 (1b/100 ft2) after 10 s where for the reference mud was 11 (1b/100 ft2).

The gel strength after 10 min varies from 16, 18 (1b/100 ft2) for the new viscosifier and was 12 (1b/100 ft2) for the mud reference.

*Thixotropy*: Thixotropy of the new viscosifiers was 2 and 3 (1b/100 ft2) where for MR was 1 (1b/100 ft2). The results of gel strength and thixotropy of the new prepared viscosifiers were within the acceptable range compared to the MR.

### 6.2. Effect of temperature on rheological properties

Rheological properties varied with temperature for both oil-based mud formulated with polymeric nano composite C, G and reference mud sample R. Fig. 11 shows the decrease of rheological properties as temperature increased from 60 °F to 200 °F.

For (M.R) mud: AV decreased from 33 cp to 13 cp.
PV decreased from 26 cp to 11 cp.
Yp decreased from 20 (1b/100 ft2) to 5 (1b/100 ft2).
For (M.C) mud: AV decreased from 70 cp to 20 cp.
PV decreased from 58 cp to 17 cp.
Yp decreased from 24 (1b/100 ft2) to 6 (1b/100 ft2).
For (M.G) mud: AV decreased from 66 cp to 28 cp.
PV decreased from 50 cp to 23 cp.
Yp decreased from 32 (1b/100 ft2) to 12 (1b/100 ft2).

### 6.3. Effect of temperature on Gel strength

Fig. 12 illustrates the gel strength of oil-based mud formulated with polymeric nano composite C, G and reference mud sample R.

For (M.R) mud: G10 s decreased from 11 (1b/100 ft2) to 4 (1b/100 ft2).
G 10 min deceased from 12 (1b/100 ft2) to 6 (1b/100 ft2).
For (M.C) mud: G10 s decreased from 14 (1b/100 ft2) to 5 (1b/100 ft2).
G 10 min deceased from 16 (1b/100 ft2) to 7 (1b/100 ft2).
For (M.G) mud: G10 s decreased from 15 (1b/100 ft2) to 2 (1b/100 ft2).
G 10 min deceased from 18 (1b/100 ft2) to 4 (1b/100 ft2).

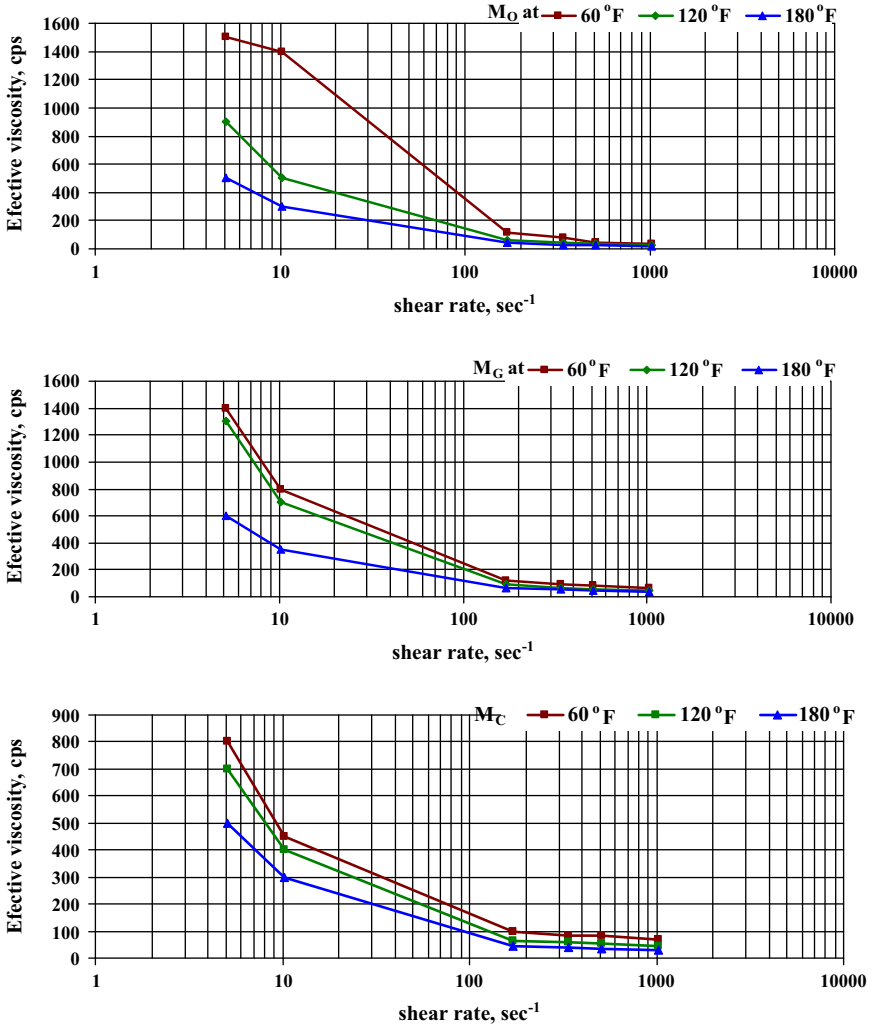


**Figure 14** Effective viscosity of $M_o$, $M_G$ and $M_C$ at 60 °F, 120 °F and 180 °F.

### 6.4. Thixotropy

Table 1 shows the thixotropy of oil-based mud with the new viscosifier C and G compared to reference oil-based mud MR as the temperature increased from 60 °F to 200 °F. Data show that the thixotropy was not affected by the increase in temperature for all the mud formulations MC, MG and MR.

And this indicates the stability of the mud even at high temperature.

## 7. Shear rate-shear stress relationship

Shear rate-shear stress relationship at different temperatures 60 °F, 120 °F, 180 °F was studied and illustrated in Fig. 13. The value of shear stress decreased as shear rate decreased for the oil-based mud treated with carbon-nano composite Mc and graphene nanoplates MG and compared to the reference conventional-based mud Mo at the same temperature.

At 60 °F: The value of shear stress decreases from 149 to 5.3 as shear rate decreases from 1020 $s^{-1}$ to 5.1 $s^{-1}$.

At 120 °F: The value of shear stress decreases from 96 to 7.4 as shear rate decreases from 1020 $s^{-1}$ to 5.1 $s^{-1}$.

At 180 °F: The value of shear stress decreases from (to) from Mc and from (64 to 5.3) for Mg as shear rate decreases from 1020 $s^{-1}$ to 5.1 $s^{-1}$. These results are similar to the result obtained in case of the field mud Mo with the conventional viscosifier.

### 7.1. Effective viscosity

A log–log graph paper for plotting viscosity for the mud versus the shear rate is represented graphically in Fig. 14, vertical lines show the rpm equivalents of shear rates in sec, drilling fluids are usual pseudo–plastic, i.e shear thinning fluids.

Test results illustrated that effective viscosity of the mud Mc and Mg decreases with increasing shear rate. This result is similar to field Mo mud formulated with conventional viscosifier.

### 7.2. Filtration properties

Table 2 reveals that the high pressure – high temperature filter loss at 250 °F for the oil-based mud formulated with the new prepared polymeric nano composite C and G and the reference oil-based mud MR. From the filtration result we can conclude that filter loss of MG (7 ml) is less than that of MC (8 ml) and MR (9 ml), so the polymeric graphene nanoplatelets (G) have great effect in reducing the filter loss of the mud than polymeric nano composite carbon nano tube (C).

**Table 2** High pressure–high temperature filter loss.

| Mud formulation | Filter loss ml |
|---|---|
| MR | 9 |
| MC | 8 |
| MG | 7 |

**Table 3** Electrical stability (mv) of the formulated mud.

| Mud | Electrical stability |
|---|---|
| MR | 750 |
| MC | 750 |
| MG | 750 |

**Table 4** The flow behavior index ($n$) and consistency index (K).

| Mud type | Dial reading at 600 rpm | Dial reading at 300 rpm | Flow behavior index ($n$) dimensionless | Consistency index (K) lb $s^n/ft^2$ |
|---|---|---|---|---|
| Mo | 66 | 46 | 0.521 | 1.793 |
| Mc | 140 | 32 | 0.771 | 1.669 |
| Mg | 132 | 32 | 0.686 | 1.136 |

### 7.3. Electrical stability

The break down voltage in (mv) was measured for the oil-based mud formulated with the new prepared polymeric nano composite C and G compared to the oil-based reference mud (R), Table 3 illustrates that the value of electrical stability (mv) of MG and MC is equal to MC.

### 7.4. Application of the power law model to the rotary viscometer data

The flow behavior index ($n$) and consistency index ($K$) values are calculated according to the power law model Herschel-Buckley model and are given by: $\tau = \tau_0 + k\cdot\gamma^n$ [34,35]

$\tau$ = shear stress
$\tau_0$ = yield stress or yield point
$K$ = the consistency factor (viscosity in case of a newtonian or bingham fluid)
$\gamma$ = share rate
$n$ = the power of low exponent (rate index) or flow behavior.

Table 4 illustrates the flow behavior index ($n$) and the consistency index ($k$) of MG and MC compared to $M_o$.

## References

[1] M. Gröndahl, L. Eriksson, P. Gatenholm, Biomacromolecules 5 (2004) 1528.
[2] J.U. Rhim, K.W.N.G. Perry, Science 47 (2007) 411.
[3] A. Sorrentino et al, Trends Food Sci. Technol. 18 (2007) 84.
[4] R.N. Tharanathan, Trends Food Sci. Technol. 14 (2003) 71.
[5] J.K. Pandey, A.P. Kumar, M. Misra, A.K. Mohanty, L.T. Drzal, R.P. Singh, Nanosci. Nanotechnol. 5 (2005) 497.
[6] A. Khare, S.J. Deshmukh, Plastic Film Sheet. 22 (2006) 193.
[7] M.J. Kawasumi, Polym. Sci, Polym. Chem. 42 (2004) 819.
[8] M. Alexandre, P. Dubois, Mater. Sci. Eng. 28 (2000) 1.
[9] L. Cabedo et al, Macromol. Symp. 233 (2006) 191.
[10] A. Lopez-Rubio et al, Trends Food Sci. Technol. 17 (2006) 567.
[11] M.N.V.R. Kumar, React. Funct. Polym. 46 (2000) 1.

[12] G. Kale, T. Kijchavengkul, R. Auras, M. Rubino, S.E. Selke, S. P. Singh, Macromol. Biosci. 7 (2007) 255.
[13] L. Petersson, K. Oksman, Compos. Sci. Technol. 66 (2006) 2187.
[14] C. Bastioli, Starch/Stärke 53 (2001) 351.
[15] J.M. Krochta, C.L.C. De-Mulder, Food Technol. 51 (1997) 61.
[16] K.S. Miller, J.M. Krochta, Trends Food Sci. Technol. 8 (1997) 228.
[17] A. Rindlav-Westling, M. Stading, A.M. Hermansson, P. Gatenholm, Polymers 36 (1998) 217.
[18] B.L. Butler, P.J. Vergano, R.F. Testin, J.M. Bunn, J.L. Wiles, Food Sci. 61 (1996) 953.
[19] D. Elliott, Materials: The life of a carton, Packaging News, 2010 [Online]. http://www.packagingnews.co.uk/news/materials-the-life-of-a-carton/.
[20] R. Caenn, G.V. Chillinger, J. Petrol. Sci. Eng. 14 (3–4) (1996) 221–230.
[21] G.V. Chillingarian, P. Vorbuter, Drilling Fluids, Elsevier Scientific Publishing, 1981.
[22] G.E. Van, J. Petrol. Sci. Eng. 286 (5) (2001) 275–287.
[23] H.C.H. Darley, G.G. Gary, Composition and Properties of Drilling and Completion Fluids, Fifth ed., Gulf Publishing Co, Houston, TX, 1998, pp. 642.
[24] D. Denney, in: J. Petrol. Technol. V57 (7) (2005) 61–63.
[25] R.L. Brazzel, "Multi-component drilling fluid additive and drilling fluid system incorporating the additive", USA Patent, 7, December 22, 2009, 635–667.
[26] M. Melbouci, A.C. Sau, "Water-based drilling fluids," U.S.A. Patent 7, 384, 892, June 10, (2008).
[27] S. Pål, "Drilling Fluids Engineering", first ed., Pålskalle & Ventus Publishing APS, 2011, pp. 120–126, ISBN: 978-87-7681-929-3.
[28] J. Anon, in: Offshore Technol. V10 (2) (2002) 12-14–15.
[29] Anon, in: J. Petrol. Technol. 50 (11) (1998) 67.
[30] L. Long, Sun Jin-Sheng, Xu Xian-Guang, Ma Cha, Yang Yu-Ping, Yuan Xu-Bo, Study and application of nano materials in drilling fluids, J. Adv. Mater. Res. 535-537 (2012) 323–328.
[31] American Petroleum Institute API RP 13B–1, "Standard Practice for Field Testing Water-based Drilling Fluids" Recommended practice, second ed., pp. 17–19, Washington D. C., 1997.
[32] Oil Companies Materials Association (OCMA), Specification No. DFCP-4, Drilling Fluid Materials, The Institute of Petroleum, London, 1983, pp. 5–9.
[33] F.A.D.L. Samar, (M.Sc., thesis), The American University in Cairo, Egypt, 2013.
[34] M.J. Davison, S. Clary, A. Saases, M. Allouche, D. Bodline, A. V. Nguyen, Rheology of various drilling fluid systems under deep water drilling conditions and the importance of accurate predictions of down hole fluid hydraulics SPE paper (56632), SPE annual technical conference and exhibition hold in Houston, Tex as, 3–6 October 1999.
[35] J. Hermoso, F. Martinez–Boza, C. Gallegas, Influence of viscosity modifier nature and concentration in the viscous flow behavior of oil-based drilling fluids at high pressure, J Appl. Clay Sci. 87 (2014) 14–21.